

# How $^{13}\text{C}$ NMR of N-heterocyclic Carbenes selectively probes $\sigma$ donation in Gold(I) complexes

D. Marchione<sup>a</sup>, M. Izquierdo<sup>b,c</sup>, G. Bistoni<sup>d</sup>,  
R. W. A. Havenith<sup>e,f</sup>, A. Macchioni<sup>g</sup>, D. Zuccaccia<sup>h</sup>,  
F. Tarantelli<sup>\*,g,i</sup>, L. Belpassi<sup>\*,i</sup>

<sup>a</sup> *Science Division, Jet Propulsion Laboratory,*

*California Institute of Technology, Pasadena, CA 91109, USA.*

<sup>b</sup> *Theoretical Chemistry, Zernike Institute for Advanced Materials  
University of Groningen, The Netherlands.*

<sup>c</sup> *Software for Chemistry and Materials, Theoretical Chemistry  
Vrije University, De Boelelaan 1083, 1081 HV Amsterdam, The Netherlands*

<sup>d</sup> *Max Planck Institute for Chemical Energy Conversion, Mülheim an der Ruhr, Germany*

<sup>e</sup> *Stratingh Institute for Chemistry, University of Groningen  
Nijenborgh 4, 9747 AG Groningen, The Netherlands.*

<sup>f</sup> *Department of Inorganic and Physical Chemistry, University of Ghent,  
Krijgslaan 281 (S3), B-9000 Gent, Belgium.*

<sup>g</sup> *Dipartimento di Chimica, Biologia e Biotecnologie,  
Università di Perugia, Italy.*

<sup>h</sup> *Dipartimento di Scienze Agroalimentari, Ambientali e Animali,  
Sezione di Chimica, Università di Udine, Italy.*

<sup>i</sup> *Istituto di Scienze e Tecnologie Molecolari del CNR  
(CNR-ISTM), Via Elce di Sotto 8, 06123 Perugia, Italy.*

## Abstract

The Dewar-Chatt-Duncanson (DCD) model provides a successful theoretical framework to describe the nature of the chemical bond in transition metal compounds and is especially useful in structural chemistry and catalysis. However, how to actually measure its constituents (substrate to metal donation and metal to substrate back-donation) is yet uncertain. Recently, we demonstrated that the DCD components can be neatly disentangled and the  $\pi$  back-donation component put in strict correlation with some experimental observables. In the present work we make a further crucial step forward, showing that, in a large set of charged and neutral N-heterocyclic carbene complexes of gold(I), a specific component of the NMR chemical shift tensor of the carbenic carbon provides a selective measure of the  $\sigma$  donation. This work opens the possibility i) to characterize unambiguously the electronic structure of a metal fragment ( $\text{LAu(I)}^{n+/0}$  in this case) by actually measuring its  $\sigma$  withdrawing ability, ii) to quickly establish a comparative trend for the ligand trans effect, and iii) to achieve a more rigorous control of the ligand electronic effect, which is a key aspect for the design of new catalysts and metal complexes.

## Introduction

The Dewar-Chat-Duncanson (DCD) bonding model [1, 2] was introduced in 1951 for rationalizing the coordination of olefines to coinage metals. It describes the metal-ligand bond simply as a donor-acceptor interaction (the ligand-to-metal donation and the metal-to-ligand back-donation). Nowadays, it has become a standard to describe the coordination bond in transition metal complexes and is commonly used for describing the electronic properties of ligands and/or metal fragments. It finds widespread application in homogeneous catalysis, where the rationalization of the electronic ligand effect in terms of the DCD components is used as a key ingredient towards a more rational design of new catalysts. [3, 4, 5]

Experimental techniques provide valuable information on the net donor-acceptor character of ligands and/or metallic fragments (consider for instance the Tolman or Lever parameters [6, 7, 8]), but if and how an observable depends on the individual DCD bonding components—and can in turn be used as a useful probe to deepen the understanding of the nature and properties of complexes—remains very difficult to ascertain. [9, 10, 11] Recently, building on a clear-cut theoretical definition of the donation and back-donation charges based on a suitable decomposition of the so called Charge-Displacement function (CDF), [12, 13] we gave a first important proof that the donation and back-donation components of the DCD model can be unambiguously disentangled and put in very tight correlation with experimental observables. [14] This promising result motivated us to look for experimental observables able to single out a specific component of the DCD model. We mainly focused on linear complexes of gold(I), in which an unsaturated carbon interacts with a gold-ligand moiety ( $[\text{LAu}]^{n+/0}$ ), (such complexes play a well-established role in gold catalysis [5, 15, 16, 17]). We proved that the back-donation component in the Au-C bond is in strict correlation with, for example, the variation of rotational barrier of the C-N bond of a nitrogen acyclic carbene ligand (NAC), which can be measured with NMR spectroscopic techniques, in complexes of formula  $[\text{(L)Au(I)(NAC)}]$  [18], or with the geometric perturbation of the cyclopropyl ring in  $[\text{LAu(S)}]^{n+}$  ( $\text{S} = \text{cyclopropyl(methoxy)carbene}$ ) complexes. [19, 20] We have recently shown how back-donation quantitatively controls the CO stretching response in classical and non-classical metal carbonyl complexes. [21]

Proceeding along this research line, we study here the fundamental question if and how the  $\sigma$  donation component of the DCD model can be selectively measured. We demonstrate that  $^{13}\text{C}$ -NMR (and specifically one of the principal components of the shielding tensor) of the carbenic carbon of Arduengo-type N-heterocyclic carbenes (NHCs) selectively probes the  $\sigma$  donation component

(NHC→AuL) of the bond in complexes of formula [(L)Au(I)(NHC)]<sup>n+/0</sup>.

The NMR spectroscopy of NHCs has attracted significant attention since their discovery [22, 23, 24, 25]. In his seminal work, Arduengo et al. [26], using solid state NMR techniques (<sup>13</sup>C CP/MAS) and pioneering calculations, cleverly showed that the strongly deshielded isotropic chemical shift ( $\delta_{iso}$ ) signal of free NHCs (for example,  $\delta_{iso}$  for the five-membered NHCs is 210-220 ppm [24]) is dominated by a single principal component of the shielding tensor. In the reference system illustrated in Fig. 1, the isotropic shielding constant  $\sigma_{iso}$  is simply given by the mean of the three non-zero (diagonal) components of the tensor:  $\sigma_{iso} = (\sigma_{XX} + \sigma_{YY} + \sigma_{ZZ})/3$ , and the dominating component found by Arduengo et al. is  $\sigma_{YY}$ .

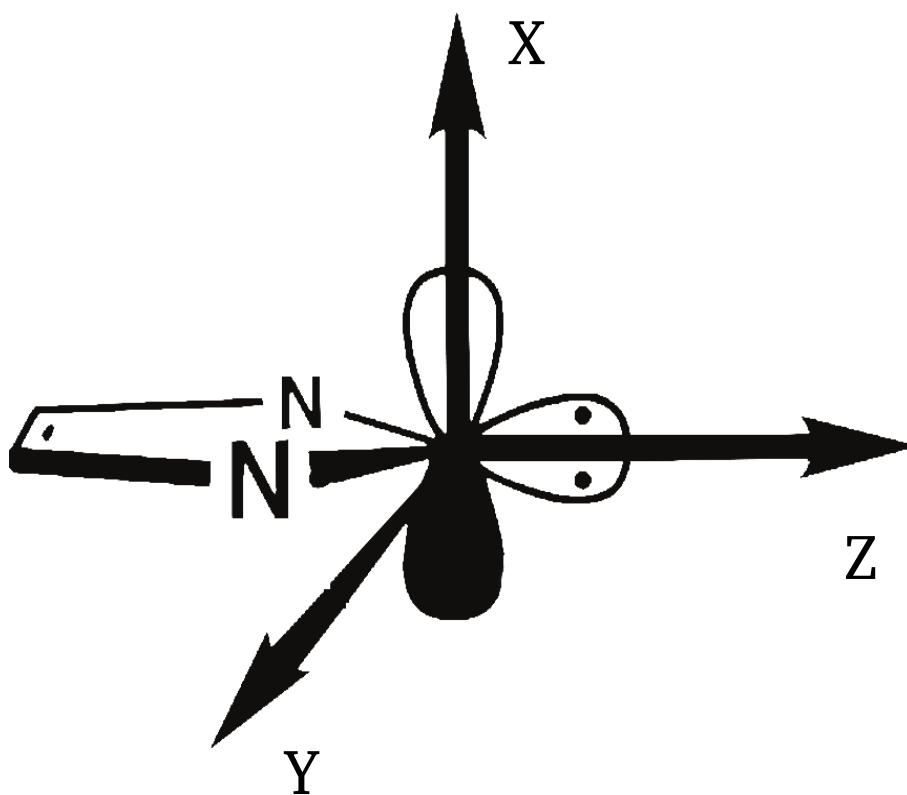


Figure 1: The principal axes of the shielding tensor used by Arduengo [26]. They identify the orthonormal reference system, centered on the carbenic carbon, in which the 3x3 chemical shielding tensor is diagonal. The Z axis is the symmetry axis of the NHC, the Y axis lies on the plane of the NHC ring, and the X axis is perpendicular to the plane in a right-handed system. Image adapted from Ref. [26].

Despite being generally considered a valuable source of information about

the electronic structure around the nuclei of interest [27, 28], experimental determinations of the NMR shielding tensor in NHC complexes are surprisingly scarce. In Table 1 we summarize the available experimental data. An interest-

Molecule	$\delta_{iso}$	$\sigma_{iso}$	$\sigma_{YY}$	$\sigma_{ZZ}$	$\sigma_{XX}$
NHC <sup>Me</sup> <sup>a</sup>	209.6	-23.2	-184(20)	9(18)	104(15)
NHC <sup>Me</sup> · H <sup>+</sup> <sup>a</sup>	137.0	49.4	45(11)	7(11)	94(11)
NHC <sup>Ph</sup> · AgCl <sup>b</sup>	184.1	2.3	-113(4)	23(4)	98(3)

Table 1: Experimental CP/MAS data (in ppm) of the isotropic chemical shift ( $\delta_{iso}$ ) and shielding tensor components ( $\sigma_{YY}$ ,  $\sigma_{ZZ}$ ,  $\sigma_{XX}$ ), with the uncertainty given in parentheses. NHC<sup>Me</sup> is 1,2,4,5-tetramethylimidazol-2-ylidene. NHC<sup>Ph</sup> is 1,3-bis(2,4,6-trimethylphenyl)-imidazol-2-ylidene. ( $\sigma_{iso}$ ) and its components  $\sigma_{YY}$ ,  $\sigma_{ZZ}$  and  $\sigma_{XX}$  have been derived from chemical shifts, consistently with Arduengo’s work[26], using  $\delta_j = \sigma_{iso}^{ref} - \sigma_j$  ( $j = iso, XX, YY, ZZ$ ) with  $\sigma_{iso}^{ref} = 186.4$ . The orientation of the principal axes is, for all systems, as that of Fig.1 for a free NHC. <sup>a</sup>data are taken from [26]. <sup>b</sup>data are taken from [29].

ing picture emerges from the analysis of Table 1.  $\sigma_{XX}$  and  $\sigma_{ZZ}$  are relatively constant (and positive), regardless of whether NHC is bare (NHC<sup>Me</sup>), in the salt (NHC<sup>Me</sup> · H<sup>+</sup>) or coordinated to a metal (NHC<sup>Ph</sup> · AgCl) [29]. Conversely, the  $\sigma_{YY}$  component varies from system to system and constitutes the main contribution to  $\sigma_{iso}$ . We underline that we can safely compare, here, the individual tensor principal components of different systems because their principal axes coincide. The orientation of the principal axes is dictated by the local symmetry at the carbene center and the three systems in the table present a C<sub>2V</sub> molecular symmetry around the carbenic carbon. The comparison of the principal components may not be so obvious in less symmetric systems (see below).

The fact that only  $\sigma_{YY}$  changes is eye-catching. This component originates from the current induced by the external magnetic field along *Y* direction (B<sub>*Y*</sub>) in the *XZ* plane, which is the plane containing the carbenic carbon lone-pair (mainly involved in the donation to the metallic fragment) and its formally empty *p<sub>x</sub>* orbital accepting the back-donation (see Fig. 1). Consequently,  $\sigma_{YY}$  puts itself forward as an ideal observable for probing the NHC bonding environment, and in principle, of the DCD bonding components. Therefore, we decided to carry out an exhaustive investigation of many NHC complexes to assess this surmise.

## Results and Discussion

Among various suitable candidate systems [24, 30], our choice fell on  $[(\text{NHC})\text{AuL}]^{n+/0}$  compounds because: a) as mentioned above, the electronic properties of metal fragment  $[\text{AuL}]^{n+/0}$  can be easily modulated by varying the ligand L [31]; b) the available experimental  $\delta_{iso}$  data show a significant dependence on the ligand, with values ranging from 204.9 to 164.6 ppm for  $[(\text{NHC}^{IPr})\text{AuH}]$  and  $[(\text{NHC}^{IPr})\text{AuNO}_3]$ , respectively (see the Exp.  $\delta_{iso}$  data in Table 2). We therefore analyzed nineteen complexes of formula  $[(\text{NHC})\text{AuL}]^{n+/0}$ , with L covering a wide range of ligands (see Fig. 2 and Table 2 for complexes labelling) from strongly electron-withdrawing ones (such as the dicationic phosphine [32]) to electron-donating ones (such as the anionic ligands).

The series includes both symmetric and unsymmetric ligands, and some of the complexes are effectively used in homogeneous catalysis [32]. In the calculations we used the imidazol-2-ylidene (simply denoted hereafter as NHC) as model carbene, whilst the ligands have been treated without simplifications. Geometries, NMR parameters and electron densities were calculated using Density Functional Theory (DFT) including relativistic effects (scalar and spin-orbit), as detailed in the section of Computational Methods. Initial efforts were made to make sure that we can reproduce the experimental trend of the available  $\delta_{iso}$ , which is an important prerequisite before conducting more detailed analysis of the shielding tensor. An excellent linear correlation ( $R^2=0.98$ ) was obtained between our calculated isotropic shielding constant and available experimental values (typically obtained in solution) of the isotropic chemical shift (data reported in Table 2, for a graphical representation see Fig.S1 in Supporting Information, SI).

From our calculations of the shielding tensor, the very important first result is that the principal axes directions of the shielding tensor do not show appreciable deviations from those of free NHC (shown in Fig. 1) in the whole  $[(\text{NHC})\text{AuL}]^{n+/0}$  series (the largest deviation, found for  $[\text{NHC}\text{AuNO}_3]$ , remains below 2 degrees). This represents a key aspect, as it means that, independent of the ligand (symmetric or unsymmetric), the carbenic carbon maintains its local symmetry practically unaltered, presumably because of the rigid structure of the NHC ring. Consequently, the values of the principal components of the shielding tensor (the actual quantities measured in solid state NMR spectroscopy) can be safely labelled and compared between different complexes. Moreover, and importantly for our purpose,  $\sigma_{YY}$  maintains its physical interpretation unaltered, retaining its unique vantage point within the molecular framework and probing the electronic structure exactly in the NHC-Au bonding region.

In view of the above considerations, the results of our calculations, shown



**L** = 1,3-bis(2,6-di-isopropylphenyl)-imidazol-2-ylidene (**NHC**<sup>IPr</sup>),  
 tert-butyl isocyanide (**CNR**), **Br**<sup>-</sup>, **2-hexyne**, **Cl**<sup>-</sup>, **CO**, **NO**<sub>3</sub><sup>-</sup>, **Xe**, **P(Ph)**<sub>3</sub>,  
**H**<sup>-</sup>, phenyl<sup>-</sup> (**Ph**<sup>-</sup>), **P(OPh)**<sub>3</sub>, Pyridine (**Py**), **TTP**, **TMP**, **PArF**, **DPbi**, **ACPP**

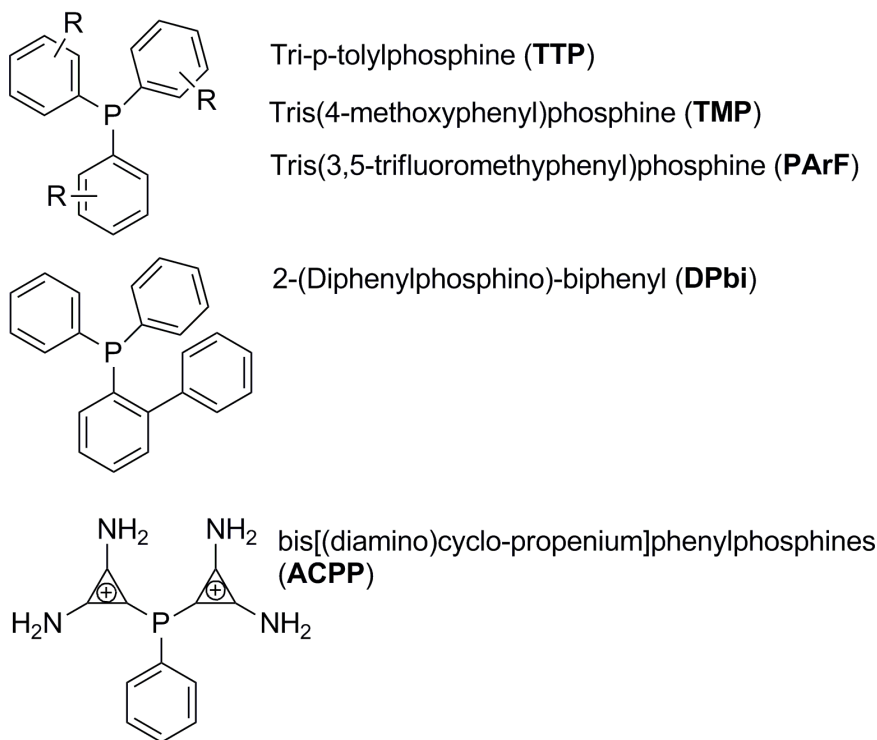


Figure 2: Molecular structures and abbreviations of the ligands considered in this work. The labelling of the relative  $[(\text{NHC})\text{AuL}]^{n+/0}$  complexes is given in Tab. 2

in Fig.3 (for the numerical values, see Table S1 in the SI), are illuminating.

We see that the  $\sigma_{YY}$  component depends strongly on the nature of the metal fragment  $[\text{AuL}]^{n+/0}$  and accounts, essentially alone, for the whole variation of the isotropic shielding constant in the entire series of complexes. The other two components,  $\sigma_{XX}$  and  $\sigma_{ZZ}$ , give almost constant contributions (negative and positive, respectively) which tend to cancel each other. We have thus proved the generality of  $\sigma_{YY}$  dominance and we now wish to quantitatively ascertain whether some correlation can be established between  $\sigma_{YY}$  (or  $\sigma_{iso}$ ) and the DCD components of the Au-C bond.

We base our investigation on the well-established definition of the dona-

Compound	Label	Exp. $\delta_{iso}$ (ppm)	Calc. $\sigma_{iso}$ (ppm)
NHC	nhc	220.6 <sup>a</sup> [24]	0
NHC·H <sup>+</sup>	h <sup>+</sup>	132.2 <sup>b</sup> [24]	93.6
(NHC)AuH	1	204.9 <sup>a</sup> [33]	17.2
(NHC)AuPh	2	198.5 <sup>a</sup> [34]	24.4
[(NHC)AuP(OPh) <sub>3</sub> ] <sup>+</sup>	3	185.2 <sup>c</sup> [35]	42.7
[(NHC)Au(NHC <sup><i>I</i>Pr</sup> )] <sup>+</sup>	4	184.2 <sup>c</sup> [36]	44.6
[(NHC)Au(CNR)] <sup>+</sup>	5	178.3 <sup>c</sup> [37]	49.5
(NHC)AuBr	6	179.0 <sup>c</sup> [38]	48.2
[(NHC)Au(2-hexyne)] <sup>+</sup>	7	177.5 <sup>d</sup> [39]	52.5
(NHC)AuCl	8	175.5 <sup>c</sup> [40]	49.6
[(NHC)Au(CO)] <sup>+</sup>	9	174.6 <sup>d</sup> [41]	55.0
[(NHC)AuPy] <sup>+</sup>	10	167.1 <sup>c</sup> [42]	63.5
(NHC)AuNO <sub>3</sub>	11	164.9 <sup>d</sup> [43]	57.6
[(NHC)Au(ACPP)] <sup>3+</sup>	12	-	55.8
[(NHC)Au(DPbi)] <sup>+</sup>	13	-	40.9
[(NHC)Au(PArF)] <sup>+</sup>	14	-	44.7
[(NHC)Au(PPh) <sub>3</sub> ] <sup>+</sup>	15	188.2 <sup>c</sup> [44]	40.1
[(NHC)Au(TTP)] <sup>+</sup>	16	-	39.1
[(NHC)Au(TMP)] <sup>+</sup>	17	-	38.2
[(NHC)AuXe] <sup>+</sup>	18	-	71.2
[(NHC)Au] <sup>+</sup>	19	-	102.3

Table 2: Experimental NMR isotropic chemical shift measured in solution ( $\delta_{iso}$ ) for the [(NHC<sup>*I*Pr</sup>)AuL]<sup>*n*+/*0*</sup> and the calculated isotropic shielding ( $\sigma_{iso}$ ) for carbenic carbon in [(NHC)AuL]<sup>*n*+/*0*</sup>. Calculated data are reported with respect to the free NHC, chosen as arbitrary zero. Measurements are in solution relative to TMS. <sup>a</sup> d<sub>6</sub>-benzene, <sup>b</sup> DMSO, <sup>c</sup>CDCl<sub>3</sub> and <sup>d</sup> CD<sub>2</sub>Cl<sub>2</sub>. The [(NHC)AuL]<sup>*n*+/*0*</sup> systems are numerically labeled from 1 to 19.

tion and back-donation charges provided by the analysis of the CDF [13, 14] (see Computational Methods section for details). In particular, we employ the recent extension of the method, referred to as CD-NOCV [45], based on the Natural Orbitals for the Chemical Valence (NOCV) theory [46], that overcomes the symmetry limitations of the original method, as some of the systems studied here do not possess any suitable symmetry. We recall that the approach is based on the decomposition of a function of the electron density rearrangement (the CDF) occurring upon formation of the complex ([NHC)AuL]<sup>*n*+/*0*</sup>

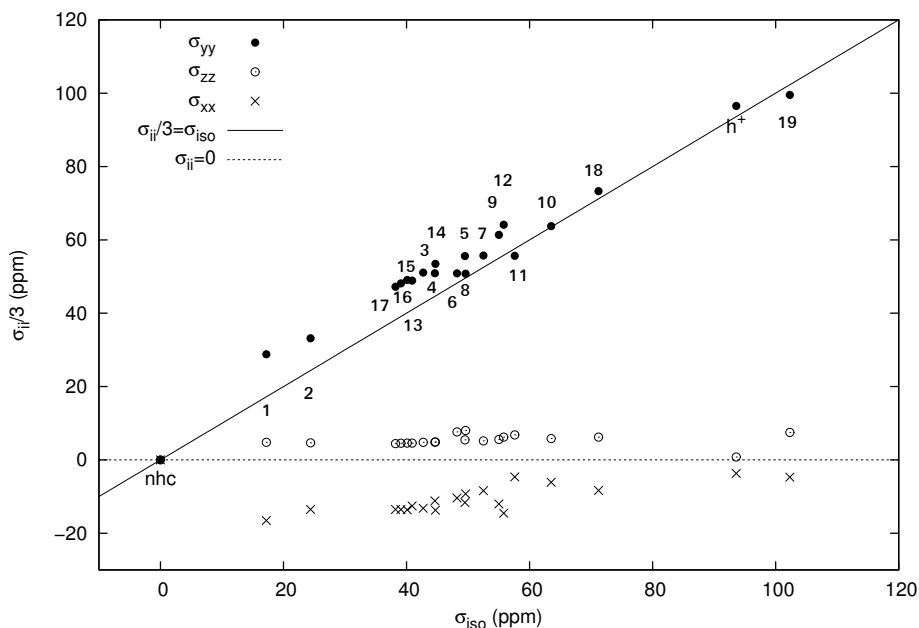


Figure 3: Decomposition of the computed isotropic shielding  $\sigma_{iso}$  in its principal components ( $\sigma_{XX}$ ,  $\sigma_{YY}$ ,  $\sigma_{ZZ}$ ). All values are relative to the values for free NHC (label "nhc"). Thus the dashed-line represents the limit case of a null change with respect to free NHC, while the solid line corresponds to a single component accounting for the whole  $\sigma_{iso}$  change.

in this case) from two fragments (NHC and  $[\text{AuL}]^{n+/0}$ ), and the donation and back-donation charge transfers ( $CT_{\sigma_{don}}$  and  $CT_{\pi}$ , respectively) are given by the value of the corresponding CDFs at a suitable inter-fragment boundary point. An illustrative example is discussed in Fig. S2 of the SI, with the numerical results summarized in Table S2 of the SI.

Fig. 4 shows that a good linear correlation does indeed exist for all complexes between the  $\sigma$  donation and  $\sigma_{YY}$  ( $R^2 = 0.94$ ). Compounds with larger  $\sigma_{YY}$  show larger values of  $CT_{\sigma_{don}}$  (larger  $\sigma$  acidity of the  $[\text{AuL}]^{n+/0}$  moiety) and vice versa. The crucial point to note is that this correlation appears to be very selective, i.e.  $\sigma_{YY}$  selectively probes  $\sigma$  donation, and not the other DCD components. Indeed, as Fig. 4 shows, the correlation between  $\sigma_{YY}$  and the total CT is instead very poor ( $R^2=0.58$ ). It is further interesting to report that the most deviant data in the plot are due to those systems presenting a significant out-of-plane ( $\pi_{\perp}$ ) back-donation component (see the SI). It is thus remarkable that systems with very different overall electronic properties can have very similar value of  $\sigma_{YY}$ . A striking example of this is provided by the 2-hexine and  $\text{NO}_3^-$  complexes (nos. 7 and 11, respectively). These systems

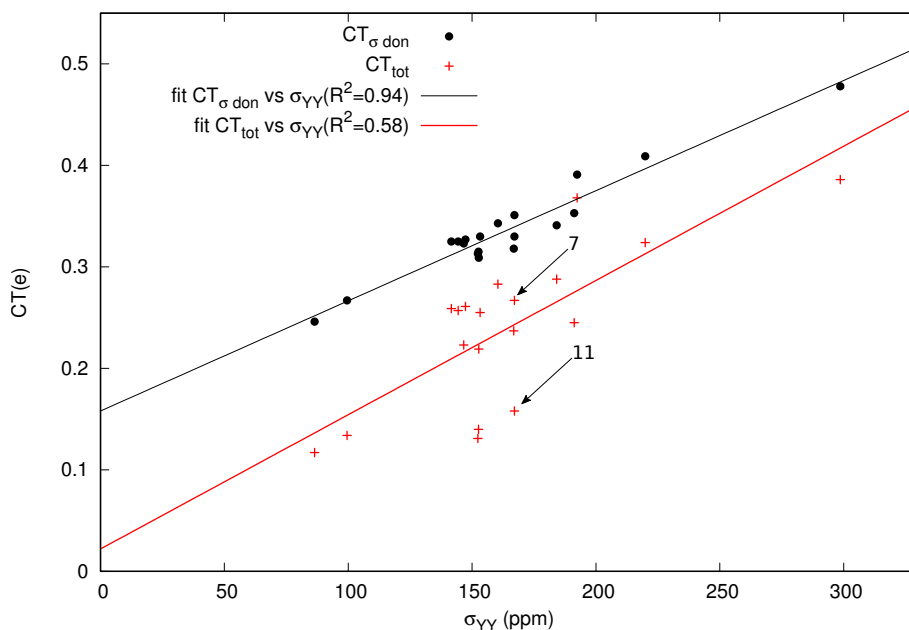


Figure 4: Black line) Linear correlation ( $R^2=0.94$ ) between the  $\sigma_{YY}$  principal component of the shielding tensor for gold(I) complexes and  $\sigma$  donation ( $CT_{\sigma_{don}}$ ). Red) Linear correlation ( $R^2=0.58$ ) between the  $\sigma_{YY}$  principal component of the shielding tensor for gold(I) complexes and the total CT ( $CT_{tot}$ ). See Table S2 and Table S3 for numerical values of the data shown. Data-points 11 and 7 highlighted by the arrows represent the 2-hexine and  $\text{NO}_3^-$  complexes (see text).

have practically the same  $\sigma_{YY}$  (167 ppm) while net CT (from NHC to  $[\text{AuL}]$ ) varies significantly (0.27 and 0.16 e, respectively). Note that the difference of 0.11 electrons transferred is about one third of the full CT range observed along the whole series. The reason of this is that the back-donation component ( $CT_{\pi_{\perp}}$ ), significantly different in the two cases, does not affect the observable  $\sigma_{YY}$ . We propose below a suitable simple interpretation of this surprising and remarkable finding.

If we look at which contributions (paramagnetic, diamagnetic and spin-orbit) mostly describes the change of  $\sigma_{YY}$  along the series, the change in the paramagnetic term (P) is unquestionably dominant (see Fig. 5, numerical data are reported in Table S3 in SI). Let us consider the expression of the paramagnetic contribution to the shielding constant (Ramsey formula [47] for a single-determinant wave function and sum-over-states approximation), it

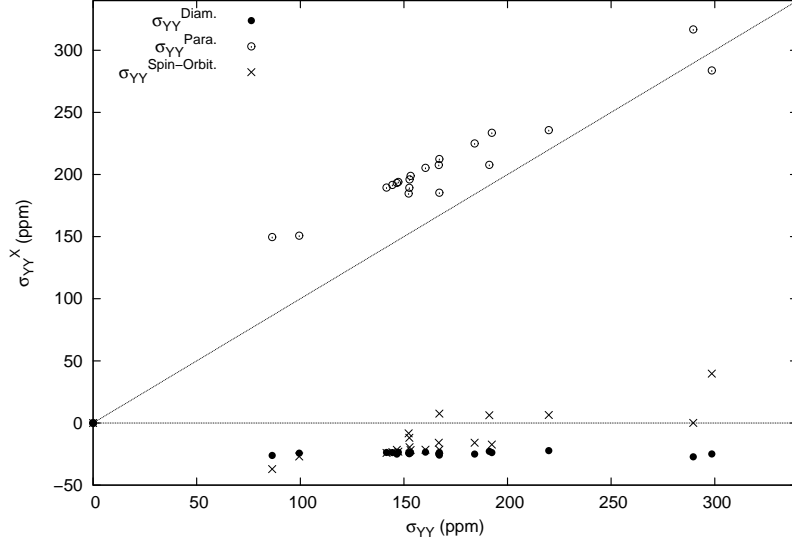


Figure 5: Contributions (in ppm) to  $\sigma_{YY}$  of diamagnetic, paramagnetic and spin-orbit terms along the  $[(\text{NHC})\text{AuL}]^{n+/0}$  series. The oblique line represents an ideal situation of a null contribution to the change for  $\sigma_{YY}$ , the horizontal line represents an ideal situation of full description to the change.

reads as

$$\sigma_{YY} = - \sum_{vir} \sum_{occ} \frac{\langle \phi_{virt} | \hat{L}_y | \phi_{occ} \rangle \langle \phi_{occ} | \hat{L}_y / r^3 | \phi_{virt} \rangle}{\epsilon_{virt} - \epsilon_{occ}} + c.c. \quad (1)$$

It depends on the occupied ( $\phi_{occ}$ ) and virtual ( $\phi_{virt}$ ) orbitals, coupled by the angular momentum operator,  $\hat{L}_y$ , and by the respective energies ( $\epsilon_{occ}$  and  $\epsilon_{virt}$ ) in the absence of the magnetic field.  $\hat{L}_y$  is the angular momentum operator along the principal axis  $Y$  with origin at the carbon nucleus position. It has the same properties as rotation operator [20]. Therefore, the contribution to  $\sigma_{YY}$  is approximately proportional to two terms: the overlap between the rotated occupied and empty orbitals ( $\langle \phi_{virt} | \hat{L}_y | \phi_{occ} \rangle$ ) and vice versa ( $\langle \phi_{occ} | \hat{L}_y / r^3 | \phi_{virt} \rangle$ ), with the latter including the radial scaling factor  $1/r^3$ . The formula can be greatly simplified by a local atomic approximation in which one retains the atomic-orbital components of the molecular orbitals pertaining to the NHC carbenic carbon:  $\phi_i(r) \sim c_{1s,i} 1s(r) + c_{2s,i} 2s(r) + c_{p_z,i} p_z(r) + c_{p_x,i} p_x(r) + c_{p_y,i} p_y(r)$ . The effect of  $\hat{L}_y$  on these

atomic orbitals is simply given by  $\hat{L}_y|s\rangle = 0$ ,  $\hat{L}_y|p_x\rangle = |p_z\rangle$ ,  $\hat{L}_y|p_y\rangle = 0$ ,  $\hat{L}_y|p_z\rangle = |p_x\rangle$  and the expression of  $\sigma_{YY}$  therefore simplifies (in local  $C_{2V}$  symmetry) to

$$\sigma_{YY} \sim - \sum_{occ} \sum_{virt} \frac{(c_{p_x, virt} \cdot c_{p_z, occ})^2}{\epsilon_{virt} - \epsilon_{occ}} - \sum_{occ} \sum_{virt} \frac{(c_{p_z, virt} \cdot c_{p_x, occ})^2}{\epsilon_{virt} - \epsilon_{occ}}. \quad (2)$$

The first term is consistent with our findings, in that it shows that  $\sigma_{YY}$  depends linearly on the square  $c_{p_z, occ}$  coefficients, which provides a measure of the change in  $\sigma$  donation: the more the NHC lone pair donates upon coordination to  $[AuL]^{n+/0}$ , the smaller will be the ground-state  $c_{p_z, occ}^2$  weights and, consequently, the smaller the contribution to  $\sigma_{YY}$ . It is further found that virtual orbitals with a large atomic  $p_x$  character (large  $c_{p_x, virt}^2$ ) typically lie at low energy, which enhances their contribution and also tends to make the variation in the relevant energy denominators relatively insignificant. The second term is in principle related to the back-donation component, in so far this is reflected by the  $p_x$  character (proportional to  $c_{p_x, occ}^2$ ) of the complex ground state orbitals. We have seen above, however, that the change in back-donation is scarcely reflected by a change in  $\sigma_{YY}$  and this simple model suggests potential reasons for this. In order to produce a significant change in  $\sigma_{YY}$ , the variation of the atomic  $p_x$  character in the ground state must be coupled with low energy virtual orbitals with a large  $p_z$  atomic character. These are not to be found, however, because low energy virtual orbitals are mainly located on the ring structure of NHC or on the metal fragment. Furthermore, the relation between back-donation and  $c_{p_x, occ}^2$  is actually found to be less stringent than one may expect at first glance: it turns out that the  $p_x$  character of occupied orbitals may be large not only because of back-donation but also - especially in charged systems where back-donation is small - because of NHC ring polarization, which brings electron charge from the nitrogens towards the carbenic carbon [48] (see for an example Fig. 6). In other words, the  $p_x$  character of the ground state orbitals is essentially "buffered" or stabilized by the presence of the ring N atoms.

## Conclusion

This work demonstrates, through an extensive computational study, that measures of the chemical shift tensor of the carbenic carbon of NHC provide a selective measure of the NHC to metal  $\sigma$  donation. We have shown this quantitatively for a large set of gold(I) complexes, but our findings and their interpretation suggest a potential wider generality, which, if verified, may open the possibility to characterize unambiguously the electronic structure of the

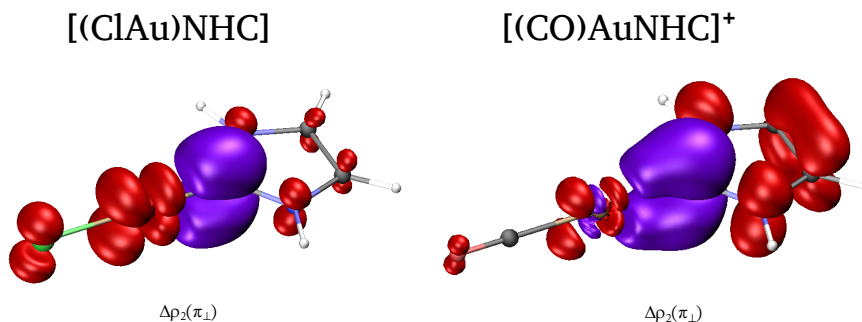


Figure 6: Electron density deformation  $\Delta\rho_{\pi_\perp}$  for [(AuCl)NHC] (and [(CO)AuNHC]<sup>+</sup>). The fragments are AuCl (and [(CO)Au]<sup>+</sup>) and NHC. Iso-density surface ( $\pm 0.0015$  e/au<sup>3</sup>) are superimposed to the molecular structure of the complex. Red surfaces (negative values) represent charge depletion regions; purple surfaces (positive values) represent accumulation regions. Noteworthy, both [(AuCl)NHC] (a neutral system) and [(CO)AuNHC]<sup>+</sup> (positively charged system) present a similar charge accumulation in the region of the carbenic carbon.

metal fragment by actually measuring its  $\sigma$  basicity and to quickly establish a comparative trend for the ligand trans effect. A simple model shows that the origin of the high selectivity of the chemical shift tensor lies in the specific nature and structure of N-heterocyclic carbenes, ever-young systems that never cease to surprise. We believe that this work represents a significant step forward for the understanding and common language of coordination chemistry, with potential feedback in catalysis. It establishes firm bases for further investigations, including new solid state NMR experiments and the extension to other metal complexes.

## Computational Methods

Geometry optimizations and electron densities were calculated with the Amsterdam Density Functional (ADF) modeling suite [49] by means of density functional theory (DFT) using the Becke's exchange functional [50] plus the LeeYangParr correlation functional [51] (BLYP). All electron triple- $\zeta$  basis sets with two polarization functions (TZ2P) and a small frozen core were used for all atoms. Relativistic effects were included by means of the zeroth-order regular approximation (ZORA) Hamiltonian. [52, 53] The nuclear magnetic resonance(NMR) shielding tensors calculations have been carried out including both scalar-relativistic and spin-orbit coupling effects in a Gauge-including atomic orbitals (GIAO) approach as implemented in ADF. [54, 55, 56]

A detailed analysis of the bonding properties in the whole series of  $[(\text{NHC})\text{AuL}]^{n+/0}$  were carried in terms of the donation and back-donation bonding components of the Dewar-Chatt-Duncanson (DCD) model. These components were computed and disentangled through the Natural Orbital for Chemical Valence-Charge Displacement (CD-NOCV) method, as recently proposed by some of us. [45] Such approach is based on the analysis of the electron density rearrangement ( $\Delta\rho$ ) occurring upon the formation of an adduct AB (the  $[(\text{NHC})\text{AuL}]^{n+/0}$  complexes in this case) from two molecular fragments A and B (NHC and  $[\text{AuL}]^{n+/0}$ ), taking as a reference the occupied orbitals of fragments, suitably orthogonalized to each other and renormalized (for details, see refs. [46, 45]). The total  $\Delta\rho$  is decomposed in contributions coming from the different NOCV pairs ( $\Delta\rho_k$ ) that can be ascribed to a DCD component on the basis of their local symmetry. Quantitative information about these charge fluxes have been singled out by evaluating the corresponding Charge Displacement Functions [12] ( $\Delta q_k(z)$ ),

$$\Delta q_k(z) = \int_{-\infty}^z dz' \int_{-\infty}^{\infty} \int_{-\infty}^{\infty} \Delta\rho_k(x, y, z'), dx dy \quad (3)$$

defined as a progressive partial integration along a suitable  $z$  axis of the integrand  $\Delta\rho_k(x, y, z')$ . The  $z$  axis is chosen to be the bond axis between the fragments, here, defined by the axis passing through nuclei positions of the carbenic carbon and gold atoms. Accordingly, the CD function at a given point  $z$  quantifies the exact amount of electron charge that, upon formation of the bond, is transferred from right to left (the direction of decreasing  $z$ ) across a plane perpendicular to the bond axis through  $z$ . Negative values of the CD function identify charge flow in the opposite direction. In order to quantify the charge transfer (CT) upon the bond formation, it is useful to fix a plausible boundary separating the fragments in the complexes. We typically choose the isodensity value representing the point on the  $z$ -axis at which equal-valued isodensity surfaces of the isolated fragments are tangent. Electron densities ( $\Delta\rho$ ,  $\Delta\rho_k$ ) were mapped on a regular grid of points using the *densf* auxiliary program provided by the ADF package. Charge displacement functions were computed using a numerical integration procedure.

## Acknowledgements

We gratefully acknowledge financial support from the MIUR (Rome, Italy), "FIRB-Futuro in ricerca" (RBFR1022UQ). D. M. clarifies that his contribution to this work has been done as a private venture and not in the author's capacity as an affiliate of the Jet Propulsion Laboratory, California Institute of Technology.

## References

- [1] J. Dewar, *B. Soc. Chim. Fr.* **1951**, *18*, C71–C79.
- [2] J. Chatt, L. Duncanson, *J. Chem.Soc.(Resumed)* **1953**, 2939–2947.
- [3] M. D. Fryzuk, *Inorg. Chem.* **2015**, *54*, 9671–9674.
- [4] J. A. Gillespie, E. Zuidema, P. W. N. M. van Leeuwen, P. C. J. Kamer, *Phosphorus Ligand Effects in Homogeneous Catalysis and Rational Catalyst Design*, John Wiley & Sons, Ltd, **2012**, pp. 1–26.
- [5] D. J. Gorin, B. D. Sherry, F. D. Toste, *Chem. Rev.* **2008**, *108*, 3351–3378.
- [6] C. A. Tolman, *Chem. Rev.* **1977**, *77*, 313–348.
- [7] A. B. P. Lever, *Inorg. Chem.* **1990**, *29*, 1271–1285.
- [8] A. B. P. Lever, *Inorg. Chem.* **1991**, *30*, 1980–1985.
- [9] O. Back, M. Henry-Ellinger, C. D. Martin, D. Martin, G. Bertrand, *Angew. Chem., Int. Ed.* **2013**, *52*, 2939–2943.
- [10] S. V. C. Vummaleti, D. J. Nelson, A. Poater, A. Gomez-Suarez, D. B. Cordes, A. M. Z. Slawin, S. P. Nolan, L. Cavallo, *Chem. Sci.* **2015**, *6*, 1895–1904.
- [11] D. M. Khramov, V. M. Lynch, C. W. Bielawski, *Organometallics* **2007**, *26*, 6042–6049.
- [12] L. Belpassi, I. Infante, F. Tarantelli, L. Visscher, *J. Am. Chem. Soc.* **2008**, *130*, 1048–1060.
- [13] N. Salvi, L. Belpassi, F. Tarantelli, *Chem. Eur. J.* **2010**, *16*, 7231–7240.
- [14] G. Bistoni, L. Belpassi, F. Tarantelli, *Angew. Chem. Int. Ed.* **2013**, *52*, 11599–11602.
- [15] L. Nunes dos Santos Comprido, J. E. M. N. Klein, G. Knizia, J. Kästner, A. S. K. Hashmi, *Angew. Chem. Int. Ed.* **2015**, *54*, 10336–10340.
- [16] R. J. Harris, R. A. Widenhoefer, *Chem. Soc. Rev.* **2016**, *45*, 4533–4551.
- [17] A. M. Echavarren, *Nat. Chem.* **2009**, *1*, 431–433.
- [18] G. Ciancaleoni, L. Biasiolo, G. Bistoni, A. Macchioni, F. Tarantelli, D. Zuccaccia, L. Belpassi, *Chem. Eur. J.* **2015**, *21*, 2467–2473.

- [19] K. M. Azzopardi, G. Bistoni, G. Ciancaleoni, F. Tarantelli, D. Zuccaccia, L. Belpassi, *Dalton Trans.* **2015**, *44*, 13999–14007.
- [20] C. M. Widdifield, R. W. Schurko, *Concepts in Magnetic Resonance Part A* **2009**, *34A*, 91–123.
- [21] G. Bistoni, S. Rampino, N. Scafuri, G. Ciancaleoni, D. Zuccaccia, L. Belpassi, F. Tarantelli, *Chem. Sci.* **2016**, *7*, 1174–1184.
- [22] K. Öfele, *J. Organomet. Chem.* **1968**, *12*, P42 – P43.
- [23] A. J. I. Arduengo, R. L. Harlow, M. Kline, *J. Am. Chem. Soc.* **1991**, *113*, 361.
- [24] D. Tapu, D. A. Dixon, C. Roe, *Chem. Rev.* **2009**, *109*, 3385–3407.
- [25] S. Guo, H. Sivaram, D. Yuan, H. V. Huynh, *Organometallics* **2013**, *32*, 3685–3696.
- [26] A. J. Arduengo, D. A. Dixon, K. K. Kumashiro, C. Lee, W. P. Power, K. W. Zilm, *J. Am. Chem. Soc.* **1994**, *116*, 6361–6367.
- [27] D. D. Laws, H.-M. L. Bitter, A. Jerschow, *Angew. Chem. Int. Ed.* **2002**, *41*, 3096–3129.
- [28] S. Halbert, C. Copéret, C. Raynaud, O. Eisenstein, *J. Am. Chem. Soc.* **2016**, *138*, 2261–2272.
- [29] T. Ramnial, C. D. Abernethy, M. D. Spicer, I. D. McKenzie, I. D. Gay, J. A. C. Clyburne, *Inorg. Chem.* **2003**, *42*, 1391–1393.
- [30] H. Jacobsen, A. Correa, A. Poater, C. Costabile, L. Cavallo, *Coord. Chem. Rev.* **2009**, *253*, 687–703, Theory and Computing in Contemporary Coordination Chemistry.
- [31] D. Marchione, L. Belpassi, G. Bistoni, A. Macchioni, F. Tarantelli, D. Zuccaccia, *Organometallics* **2014**, *33*, 4200–4208.
- [32] J. Carreras, G. Gopakumar, L. Gu, A. Gimeno, P. Linowski, J. Petuskova, W. Thiel, M. Alcarazo, *J. Am. Chem. Soc.* **2013**, *135*, 18815–18823.
- [33] E. Y. Tsui, P. Müller, J. P. Sadighi, *Angew. Chem. Int. Ed.* **2008**, *47*, 1–5.
- [34] A. S. K. Hashmi, C. Lothschütz, R. Döpp, M. Rudolph, T. D. Ramamurthi, F. Rominger, *Angew. Chem. Int. Ed.* **2009**, *48*, 8243–8246.

- [35] J. Fernandez-Gallardo, B. T. Elie, M. Sanau, M. Contel, *Chem. Commun.* **2016**, *52*, 3155–3158.
- [36] S. Gaillard, P. Nun, A. M. Z. Slawin, S. P. Nolan, *Organometallics* **2010**, *29*, 5402–5408.
- [37] L. Canovese, F. Visentin, C. Levi, V. Bertolasi, *Organometallics* **2011**, *30*, 875–883.
- [38] P. de Frémont, R. Singh, E. D. Stevens, J. Petersen, S. P. Nolan, *Organometallics* **2007**, *26*, 1376–1385.
- [39] D. Zuccaccia, L. Belpassi, L. Rocchigiani, F. Tarantelli, A. Macchioni, *Inorg. Chem.* **2010**, *49*, 3080–3082.
- [40] S. Gaillard, A. M. Z. Slawin, A. T. Bonura, E. D. Stevens, S. P. Nolan, *Organometallics* **2010**, *29*, 394–402.
- [41] P. Dash, C. and Kroll, M. Yousufuddin, H. V. R. Dias, *Chem. Commun.* **2011**, *47*, 4478–4480.
- [42] P. de Frémont, N. Marion, S. P. Nolan, *Organometallics* **2009**, *694*, 551–560.
- [43] M. Trinchillo, P. Belanzoni, L. Belpassi, L. Biasiolo, V. Busico, A. D’Amora, L. D’Amore, A. D. Zotto, F. Tarantelli, A. Tuzi, D. Zuccaccia, *Organometallics* **2016**, *35*, 641–654.
- [44] S. Gaillard, P. Nun, A. M. Z. Slawin, S. P. Nolan, *Organometallics* **2010**, *29*, 5402–5408.
- [45] G. Bistoni, S. Rampino, F. Tarantelli, L. Belpassi, *J. Chem. Phys.* **2015**, *142*, 084112.
- [46] M. Mitoraj, A. Michalak, *J. Mol. Model.* **2007**, *13*, 347–355.
- [47] N. F. Ramsey, *Phys. Rev.* **1950**, *78*, 699–703.
- [48] D. M. Andrada, N. Holzmann, T. Hamadi, G. Frenking, *Beilstein J. Org. Chem.* **2015**, *11*, 2727–2736.
- [49] ”ADF Users Guide, Release 2012.01; SCM, Theoretical Chemistry, Vrije Universiteit: Amsterdam, The Netherlands, **2012**”.
- [50] A. D. Becke, *Phys. Rev. A* **1988**, *38*, 3098–3100.

- [51] C. Lee, W. Yang, R. G. Parr, *Phys. Rev. B* **1988**, *37*, 785–789.
- [52] E. v. Lenthe, E. J. Baerends, J. G. Snijders, *J. Chem. Phys.* **1993**, *99*, 4597–4610.
- [53] E. v. Lenthe, E. J. Baerends, J. G. Snijders, *J. Chem. Phys.* **1994**, *101*, 9783–9792.
- [54] G. Schreckenbach, T. Ziegler, *J. Phys. Chem.* **1995**, *99*, 606–611.
- [55] S. K. Wolff, T. Ziegler, *J. Chem. Phys.* **1998**, *109*, 895–905.
- [56] S. K. Wolff, T. Ziegler, *J. Chem. Phys.* **1999**, *110*, 7689–7698.